Density functional studies on wurtzite piezotronic transistors: influence of different semiconductors and metals on piezoelectric charge distribution and Schottky barrier

2016 Nanotechnology 27 205204

(http://iopscience.iop.org/0957-4484/27/20/205204)

IOP Publishing Nanotechnology
Nanotechnology 27 (2016) 205204 (7pp) doi:10.1088/0957-4484/27/20/205204

Density functional studies on wurtzite piezotronic transistors: influence of different semiconductors and metals on piezoelectric charge distribution and Schottky barrier

Wei Liu[1], Aihua Zhang[1], Yan Zhang[2] and Zhong Lin Wang[1,3]

[1] Beijing Institute of Nanoenergy and Nanosystems, Chinese Academy of Sciences; National Center for Nanoscience and Technology (NCNST), Beijing, 100083, People's Republic of China
[2] Institute of Theoretical Physics, and Key Laboratory for Magnetism and Magnetic Materials of MOE, Lanzhou University, Lanzhou 730000, People's Republic of China
[3] School of Material Science and Engineering, Georgia Institute of Technology, GA 30332, USA

E-mail: wliu@binn.cas.cn and zlwang@gatech.edu

Received 12 January 2016, revised 25 February 2016
Accepted for publication 15 March 2016
Published 7 April 2016

Abstract

The mechanical–electrical coupling properties of piezoelectric semiconductors endow these materials with novel device applications in microelectromechanical systems, sensors, human–computer interfaces, etc. When an applied strain is exerted on a piezoelectric semiconductor, piezoelectric charges are generated at the surface or interface of the semiconductor, which can be utilized to control the electronic transport characteristics. This is the fundamental working mechanism of piezotronic devices, called the piezotronic effect. In the present report, a series of piezotronic transistors composed of different electrode metals and semiconductors is examined using density functional theory calculation. It is found that the influence of semiconductors on the piezotronic effect is larger than the impact of metals, and GaN and CdS are promising candidates for piezotronic and piezo-phototronic devices, respectively. The width of the piezoelectric charge distribution obtained in the present study can be used as a parameter in classical finite-element-method based simulations, which provide guidance on designing high-performance piezotronic devices.

Keywords: piezotronic effect, wurtzite materials, piezoelectric charge distribution, Schottky barrier

(Some figures may appear in colour only in the online journal)

1. Introduction

Piezotronic devices, as a kind of flexible functional electronic device, have received broad attention due to their potential in harvesting mechanical energy from the ambient environment as well as tuning transport characteristics under deformation [1]. Noncentral symmetric wurtzite materials such as ZnO, ZnS, and CdS, simultaneously featuring piezoelectric and semiconductive properties, play a central part in piezotronic devices [2, 3]. When a piezoelectric semiconductor is under an external applied strain, piezoelectric charges (*piezocharges*) are generated at a metal–semiconductor interface or a pn junction, inducing a piezoelectric polarization that can be used to 'gate' the carrier transport by tuning the local Schottky barrier. This is called piezotronics. Much effort has been devoted to fabricating various piezotronic devices, including nanogenerators [4–6], two-terminal strain gated transistors [7], electromechanical memories [8], motion/vibration sensors [9, 10], and functional integrated systems for flexible human–machine interfacing [11]. Very recently the monolayer MoS_2 has been verified to show the piezotronic effect, which broadens the field of piezotronics to

two-dimensional transition metal dichalcogenide materials [12–14]. Besides piezotronics, the new emerging fields of piezo-phototronics [15, 16] and piezo-magnetotronics [17], that utilize the external strain to control the optical and magnetic properties, respectively, have been established to realize multi-field mechanical–electrical–optical–magnetic coupling effects based on piezoelectric semiconductors. At the same time, the piezoelectric properties and transport properties of piezotronic materials and devices have been studied by both finite-element-method (FEM) and density functional theory (DFT) simulations [18–25].

Classical piezotronic theory is based on the classical semiconductor and piezoelectric theories. Using the finite element method, the piezoelectric potential distribution in ZnO nanowires [18, 19] and dynamical transport behaviors of piezotronic devices [20] have been examined. An important finding in these studies is that the piezotronic effect largely depends on the piezocharge distribution width (*piezocharge width*) at the interface or junction region [20, 21]. However, since the piezocharges distribute within several atomic layers, the accurate calculation of the piezocharge width is beyond the scope of classical theory and one must resort to quantum mechanical simulation.

Employing the density functional theory, in previous studies we have for the first time obtained the piezocharge distribution width in an Ag–ZnO–Ag piezotronic transistor [22]. For the next step, in the present study we examine the effect of different piezoelectric semiconductors and electrode metals on piezocharge width in piezotronic transistors. In addition, the modulations of Schottky barrier height (SBH) of different transistors due to the piezotronic effect are calculated. This study is important in two ways: (1) the piezocharge width obtained from the DFT simulation can be used as a parameter in classical finite-element-method based simulations of piezotronic devices to improve accuracy and (2) the comparison of the piezocharge widths and Schottky barriers between different transistors provides suggestions on which semiconductor/metal is the most suitable component for high-performance piezotronic devices.

2. Model and method

As mentioned previously, we model the metal–semiconductor–metal piezotronic transistors in the present study. To examine the effect of different electrode metals on the piezocharge width, Ag, Au, Al, and Pt (face centered cubic structure) are used in metal–ZnO–metal transistors (referred to below as Ag, Au, Al, and Pt transistors); on the other hand, to investigate the influence of different semiconductors, ZnO, ZnS, CdS, GaN, and InN (hexagonal wurtzite structure) are used in Ag–semiconductor–Ag transistors (referred to below as ZnO, ZnS, CdS, GaN, and InN transistors). For direct comparisons between the piezocharge widths of transistors composed of different semiconductors and metals, all transistors examined in the present study have similar structures. The atomic structure of the Ag–ZnO–Ag transistor (referred to as the Ag transistor in the case of different-metal transistors, and also referred to as the ZnO transistor in the case of different-semiconductor transistors), which has already been examined in previous studies [22], is shown in figure 1 as a representative structure. Figure 2(a) gives a lateral view of this transistor. In the two figures, a blue ball denotes an Ag atom, a green ball a Zn atom, and a red ball an O atom. The transistor has a hexagonal structure (refer to the black hexagonal prism in figure 1) with its *c* axis perpendicular to the Ag(111) plane and ZnO ± (0001) polar planes. In the present study, the transistor consists of four double (eight single) ZnO layers and six Ag(111) layers, as shown in figure 2(a). At the ZnO(000$\bar{1}$) −Ag(111) interface Ag atoms lie on top of O atoms, while at the ZnO(0001)–Ag(111) interface Ag atoms are accommodated in the hcp hollow sites of the ZnO(0001) polar surface [22, 26, 27]. In fact, fcc hollow sites of the ZnO(0001) polar surface are also energy favorable for Ag atoms at the ZnO(0001)–Ag(111) interface. Since the piezocharge distributions of fcc structures are similar to those of hcp structures [22], only hcp structures are adopted in the present study. For simplicity of the simulation, any defect/impurity is neglected in the model. To obtain the relaxed equilibrium transistor structures with minimum strain and lowest energy, first an optimal contact distance between ZnO and Ag electrodes (refer to *l* in figure 2(a)) is obtained without relaxing other structure parameters; then the cell constants and atomic positions are fully relaxed to eliminate the strain. An external strain (from −5% to 5%) is applied along the *c* axis by compressing/stretching the cell constant of the equilibrium transistor while keeping the fractional coordinates of all atoms fixed. Then the transistor under the strain is fully relaxed by fixing the cell constants. Similar steps are applied for the transistors composed of other semiconductors/metals.

In the calculation, the periodical boundary condition is applied in all *a*, *b*, and *c* axes of the transistors. The black box in figure 2(a) indicates the supercell of the transistor used in the periodical calculation (also refer to the red quadrangular prism in figure 1). The simulation of the transistor is performed using the Vienna *ab initio* simulation package (VASP) [28, 29] within the framework of DFT. The frozen-core projector-augmented-wave (PAW) pseudopotential [30, 31] is used for electron–ion interactions and the Perdew–

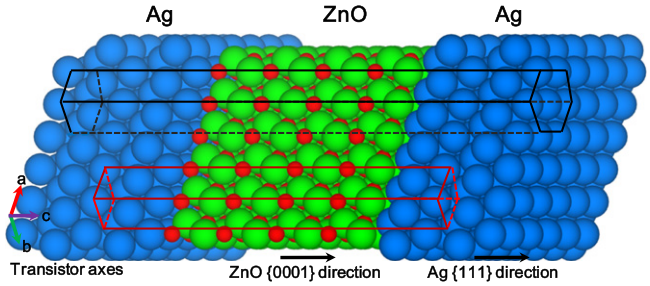

Figure 1. Atomic structure of an Ag–ZnO–Ag piezotronic transistor. A blue ball denotes an Ag atom, a green ball a Zn atom, and a red ball an O atom. The black hexagonal prism indicates the hexagonal structure of the transistor and the red quadrangular prism the transistor supercell used in the calculation.

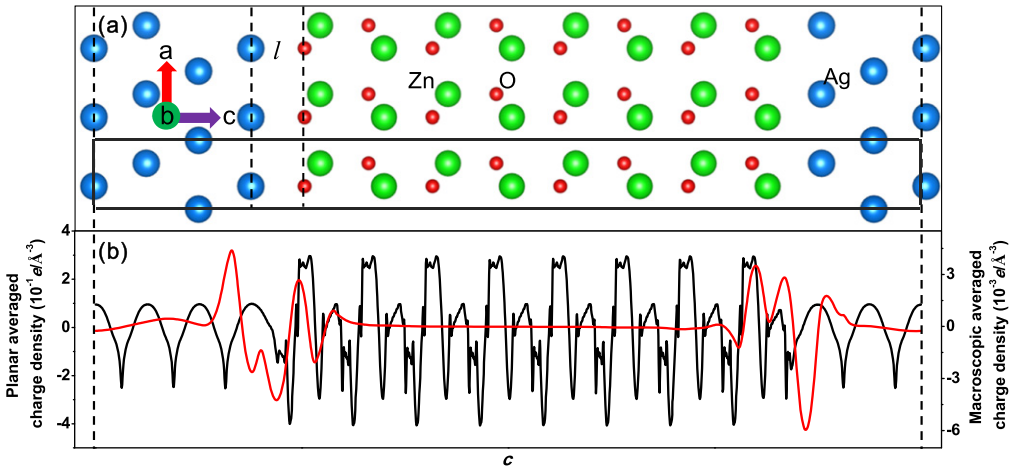

Figure 2. (a) Lateral view of an equilibrium Ag–ZnO–Ag piezotronic transistor. The supercell used in the calculation is indicated by a black box. (b) The planar averaged charge density is given by a black line. The macroscopic averaged charge density is denoted by a red line. In the unit of charge density, e denotes absolute electron charge, $e = 1.6 \times 10^{-19}$ C.

Burke–Ernzerhof (PBE) parameterization within the general gradient approximation (GGA) [32] is employed to describe the exchange–correlation functional. The single-particle Kohn–Sham wave function is expanded using the plane waves with a cutoff energy of 500 eV and sampling of the irreducible Brillouin zone for the transistor supercell is carried out with a grid of $9 \times 9 \times 3$ k points. To reduce the calculation, the adopted criterion for the Hellmann–Feynman forces in the structure optimization is 0.05 eV Å^{-1}, which is larger than the value of 0.01 eV Å^{-1} used in the previous study [22]. Such treatment leads to smaller relative movements of the atoms in the optimization, which result in different values of Schottky barriers and better linearity of the Schottky barriers versus applied strains compared with previous results for the Ag–ZnO–Ag transistor (refer to section 3.4) [22]. However, according to our examination, using a larger optimization criterion or even no structure optimization does not give qualitatively different results for piezocharge distribution width and modulation of Schottky barriers under the applied strains.

3. Results and discussion

3.1. Piezocharge distribution in an Ag–ZnO–Ag transistor

Taking an Ag–ZnO–Ag transistor as an example, the piezocharge distribution is calculated using the method in our previous theoretical work [22] in the following steps. (1) First the planar averaged electrostatic potential of the transistor along the c axis is obtained, from which the planar averaged charge density is calculated by using the Poisson equation and shown in figure 2(b) by a black line. The red line in figure 2(b) indicates the macroscopic averaged charge density, which is obtained by applying the double-macroscopic average on the planar averaged charge density [33]. (2) Then the inner Ag and ZnO regions and interface regions in the transistor are defined. The inner Ag region has width equal to the layer distance between the neighboring Ag(111) planes, the inner ZnO region has width equal to the distance between the neighboring Zn or O layers, and the interface region is sandwiched between the inner Ag region and inner ZnO region, which is from the interface Ag layer to the inner ZnO region where the macroscopic averaged charge density becomes zero. (3) According to classical piezotronic theory, the piezocharges distributed at the interface region are calculated as the difference of the planar averaged charge densities between the transistor in equilibrium and the same transistor under strain. The piezocharges of other transistors consisting of different metals or semiconductors are obtained using the same method.

Figures 3(a) and (b) give the piezocharge distributions at two transistor interfaces under the applied strains. As mentioned in the previous paragraph, the piezocharges distribute at transistor interfaces, thus the piezocharge width is equal to the width of the interface region along the c axis. Since the width of the interface region is shortened under compressive strain and lengthened under tensile strain, the calculated piezocharge width is linearly dependent on the applied strain (refer to figures 4 and 5). For the equilibrium Ag–ZnO–Ag transistor, the piezocharge width is 4.11 Å at the ZnO(000$\bar{1}$)–Ag interface and 3.68 Å at the ZnO(0001)–Ag interface, as been obtained in the previous study [22]. In the following discussion, by referring to the 'piezocharge width', we mean the 'piezocharge width in the equilibrium transistor'. Figures 3(c) and (d) show the total piezocharge per surface area (in the a–b plane) versus applied strains at ZnO(000$\bar{1}$)–Ag and ZnO(0001)–Ag interfaces, respectively. At the ZnO(000$\bar{1}$)–Ag interface, positive charges increase under compressive strain, while negative charges increase under tensile strain; on the other hand, at the ZnO(0001)–Ag interface the case is vice versa: negative charges increase under compressive strain and positive charges increase under tensile strain. All the piezocharges exist in two interface regions so the total charges in the inner Ag and ZnO regions do not depend on the strain, as shown in figures 3(c) and (d). Furthermore, to examine the convergence of our results on ZnO/Ag length, we have constructed longer

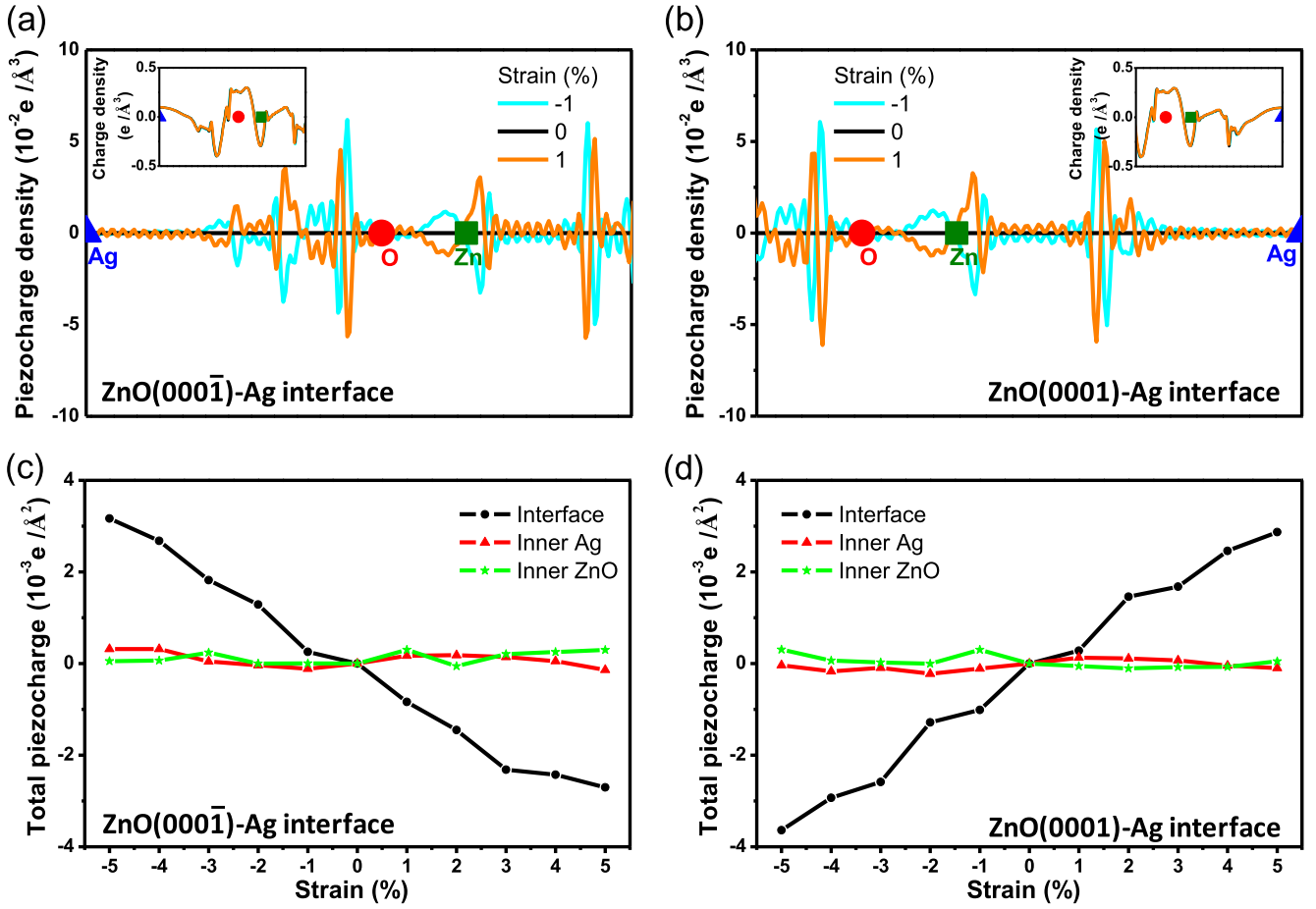

Figure 3. Piezocharge distribution at (a) the ZnO(000$\bar{1}$)–Ag interface and (b) the ZnO(0001)–Ag interface under ±1% applied strain for the Ag–ZnO–Ag piezotronic transistor. The inset in each figure is the planar averaged charge density distribution under the same strain within the interface region. The blue triangle, green square, and red circle indicate the relative positions of Ag, Zn, and O atoms, respectively, on the *c* axis. (c), (d) Total piezocharge per surface area at the ZnO(000$\bar{1}$)–Ag interface and the ZnO(0001)–Ag interface, respectively, under applied strains (−5% to 5%) for the Ag–ZnO–Ag piezotronic transistor. The total charges versus applied strains for inner Ag and ZnO regions near each interface region are also given.

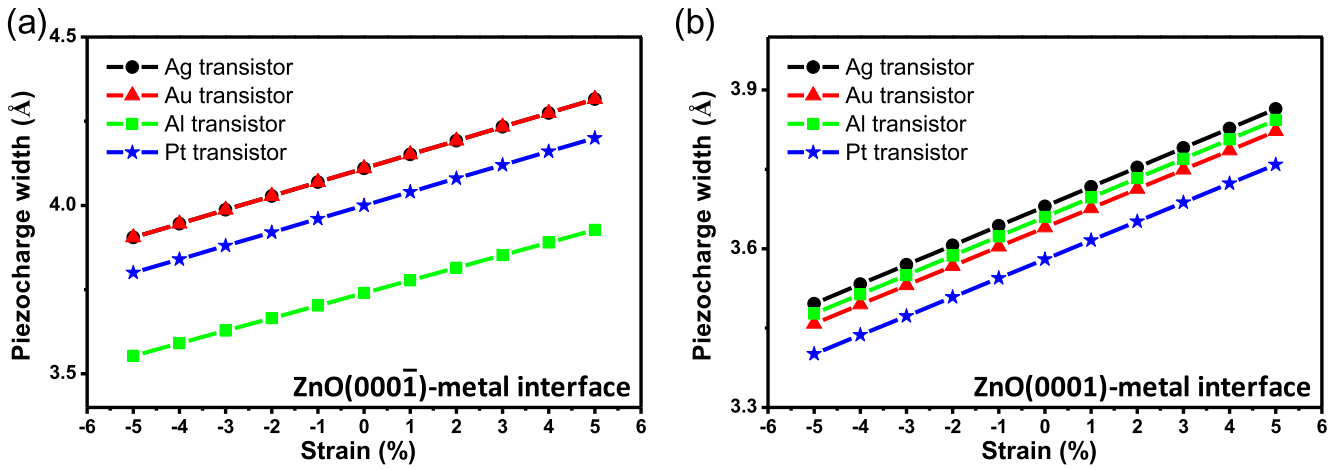

Figure 4. Piezocharge widths of the transistors composed of different metals at (a) the ZnO(000$\bar{1}$)–metal interface and (b) the ZnO(0001)–metal interface under applied strains.

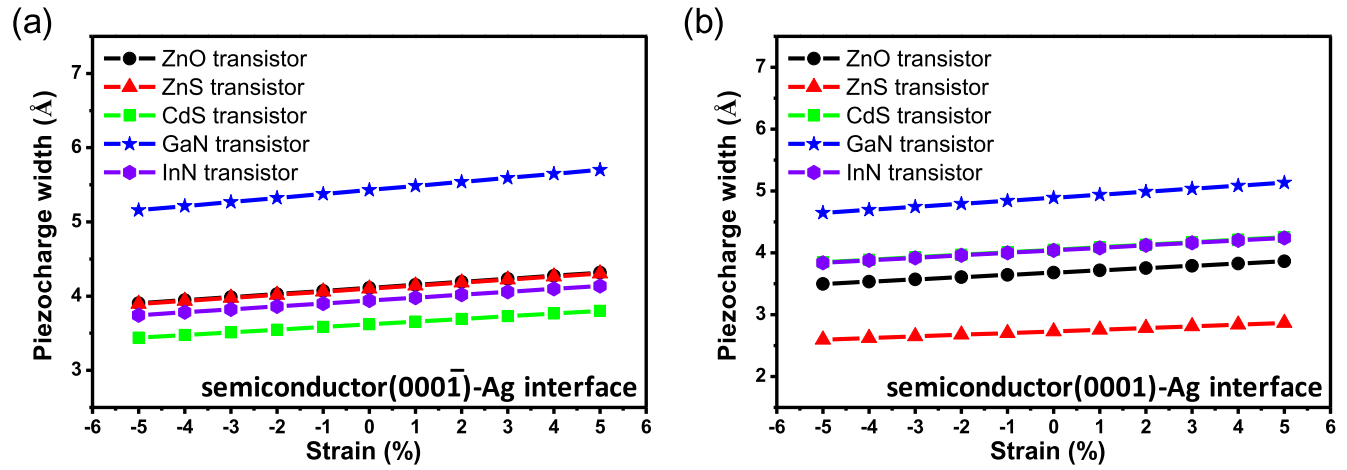

Figure 5. Piezocharge widths of the transistors composed of different semiconductors at (a) the semiconductor(000$\bar{1}$)–Ag interface and (b) the semiconductor(0001)–Ag interface under applied strains.

transistors with up to 15 double layers of ZnO and up to 12 layers of Ag. The piezocharge widths and total piezocharges of these transistors under applied strains are similar to those for the shorter ones, indicating that the transistors adopted in the present study are sufficient in length.

3.2. Effect of different metals on piezocharge distribution

Figures 4(a) and (b) show the piezocharge widths of the Ag, Au, Al, and Pt transistors under applied strains at ZnO(000$\bar{1}$) −metal and ZnO(0001)–metal interfaces, respectively. For each metal, the piezocharge region at either interface includes a layer of metal atoms and a single ZnO layer (refer to figures 3(a) and (b) for the Ag transistor). The Ag transistor has the largest piezocharge width at both interfaces (refer to the last paragraph for the piezocharge width of the Ag–ZnO–Ag transistor). At the ZnO(000$\bar{1}$)–metal interface the Al transistor has the smallest piezocharge width, which is 0.37 Å shorter than the piezocharge width of the Ag transistor, while at the ZnO(0001)–metal interface the Pt transistor has the smallest piezocharge width, which is 0.10 Å shorter than the piezocharge width of the Ag transistor. The above results indicate that the influence of the metal on the piezocharge width is not obvious (compared with the influence of different semiconductors in the next section). Since the piezocharge width is a critical parameter for the piezotronic effect, it seems that the piezotronic effect is not greatly affected by changing the metal in the device. Thus in practical experiments the concern about the metal in the devices should be on other aspects than the piezotronic effect, such as the fabrication and stability related concerns.

3.3. Effect of different semiconductors on piezocharge distribution

Piezocharge widths of the ZnO, ZnS, CdS, GaN, and InN transistors under applied strains at the semiconductor(000$\bar{1}$)–Ag and the semiconductor(0001)–Ag interfaces are given in figures 5(a) and (b), respectively. At the semiconductor(0001)–Ag interface, the piezocharge distribution regions of all transistors are similar to each other, and include a layer of Ag atoms and a single semiconductor layer. On the other hand, at the semiconductor(000$\bar{1}$)–Ag interface, although the piezocharge regions of the GaN and InN transistors are similar to those of the ZnO transistor, the piezocharge regions of the ZnS and CdS transistors are different, which include two Ag layers and an interface S layer. Compared with using different metals (refer to figure 4), the piezocharge distribution can be effectively modulated by changing the semiconductor. Among all the semiconductors used in the present study, the GaN transistor provides the largest piezocharge width at both interfaces: 5.43 Å at the semiconductor(000$\bar{1}$)–Ag interface and 4.89 Å at the semiconductor(0001)–Ag interface. The CdS transistor has the smallest piezocharge width at the semiconductor(000$\bar{1}$)−Ag interface, which is 1.81 Å shorter than the piezocharge width of the GaN transistor, while the ZnS transistor has the smallest piezocharge width at the semiconductor(0001)–Ag interface, which is 2.16 Å shorter than the piezocharge width of the GaN transistor. The largest piezocharge width of the GaN transistor is due to its longer piezocharge region inside the semiconductor, which almost extends to the second single GaN layer from the interface.

The above results suggest that the piezocharge width and thus the piezotronic effect can be effectively modulated or enhanced/attenuated by using different semiconductors. The present study supports the view that GaN is a very suitable semiconductor for highly efficient piezotronic devices due to its large piezocharge width. To best of our knowledge, there is not yet a simple method or physical constant to evaluate the piezocharge width of transistors. In fact, we have also calculated the work function of different metals and semiconductors used in the present study. Although the work function is closely related to the width of the depletion layer at the semiconductor–metal interface, we cannot find an explicit connection between the calculated work function and the piezocharge width of the transistor. Therefore, we believe the piezocharge width can be only calculated and evaluated by first-principle simulations. The DFT-calculated

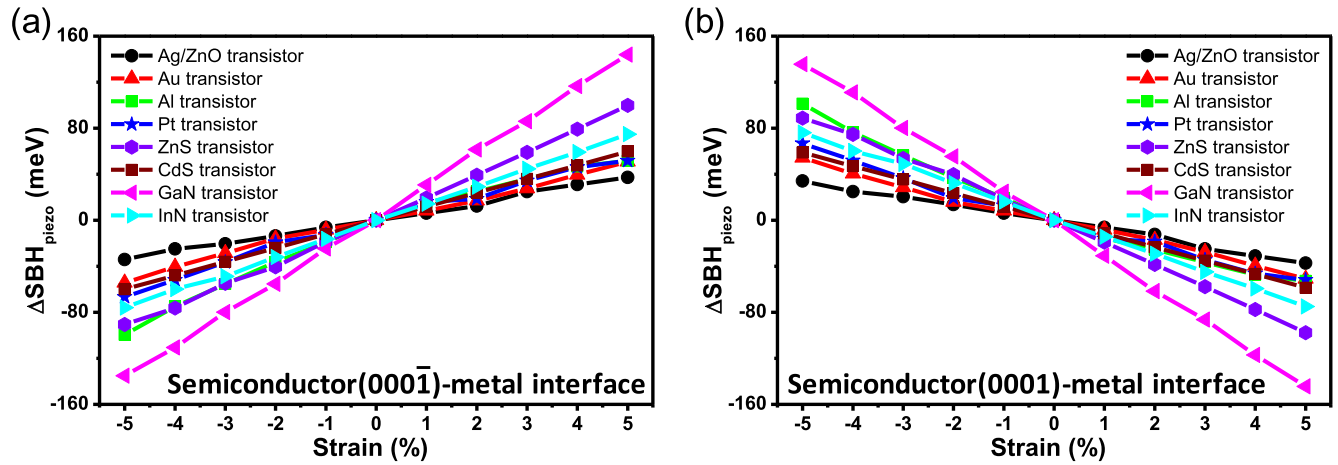

Figure 6. Modulation of SBH of different transistors under strains at (a) the semiconductor(000$\bar{1}$)–metal interface and (b) the semiconductor (0001)–metal interface.

piezocharge width in the present study can be used as a parameter in finite-element-method based simulations of piezotronic devices in order to improve the accuracy of the simulations and serve for practical device design and optimization.

3.4. Effect of different metals and semiconductors on the Schottky barrier height

The piezotronic effect employs the piezocharge to tune/control the carrier transport by changing the Schottky barrier height at the device interface under strain. Thus the modulation of SBH at the transistor interface is an important factor to evaluate the effect of different metals and semiconductors on the piezotronic effect. Following the previous studies, the modulation of SBH at metal–semiconductor interfaces due to the piezotronic effect, ΔSBH, is calculated as the change of the reference potential at the interfaces [22, 26]. The ΔSBH values of different transistors at the interfaces are shown in figure 6. For all transistors, the behaviors of ΔSBH versus applied strains are asymmetric at two interface regions: at the semiconductor(000$\bar{1}$)–metal interface ΔSBH becomes positive under tensile strain and negative under compressive strain, while at the semiconductor(0001)–metal interface the case is vice versa: ΔSBH becomes negative under tensile strain and positive under compressive strain. The asymmetric behavior of ΔSBH agrees with classical piezotronic theory. The previous experimental studies have investigated the modulation of Schottky barriers of Ag–ZnO–Ag [34] and Ag–GaN–Ag [35] transistors at the semiconductor(000$\bar{1}$)–metal interface due to the piezotronic effect and obtained the results of 4 meV and 12 meV under a 0.5% strain, which agree well with the present calculation. From the results of ΔSBH it can be found that (1) the influence of semiconductors on ΔSBH is much larger than that of metals, and (2) the GaN transistor gives the largest ΔSBH under strain and thus is a very promising semiconductor for piezotronics, both are in accordance with the conclusions from the piezocharge width. On the other hand, the CdS transistor has considerable piezocharge width, Schottky barrier modulation, and most importantly visible range optical response, which enables CdS to be a promising candidate for piezo-phototronic devices, as has been shown in recent experiments [36].

4. Conclusions

In the present study, by modeling a series of piezotronic transistors and performing the DFT calculations, we have investigated the effect of different metals and semiconductors on the piezocharge distribution and modulation of Schottky barriers under strain. It is found that the influence of the semiconductor on the piezotronic effect is much larger than the influence of the metal, and GaN and CdS are suggested as promising candidates for fabricating piezotronic and piezo-phototronic devices, respectively. The piezocharge width, which can only be obtained using first-principle simulations, is an important parameter in classical piezotronic theory and can be used in finite-element-method based simulations of piezotronic devices, while the modulations of Schottky barriers of different transistors serve as a reference for evaluating the performance of the piezotronic devices. The results of the present calculation are guidance for future experiments and hopefully will be examined.

Acknowledgments

This work was supported by the ‘Thousands Talents’ Program for a Pioneer Researcher and Innovation Team, China, and the National Natural Science Foundation of China (grant No. 51432005).

References

[1] Wu W, Pan C, Zhang Y, Wen X and Wang Z L 2013 *Nano Today* **8** 619–42

[2] Wang Z L and Song J 2006 *Science* **312** 242–6
[3] Wang Z L 2013 *Piezotronics and Piezo-Phototronics* (Berlin: Springer)
[4] Bai S, Zhang L, Xu Q, Zheng Y, Qin Y and Wang Z L 2013 *Nano Energy* **2** 749–53
[5] Kim D Y, Lee S, Lin Z H, Choi K H, Doo S G, Chang H, Leem J Y, Wang Z L and Kim S O 2014 *Nano Energy* **9** 101–11
[6] Zhang Y *et al* 2016 *ACS Appl. Mater. Interfaces* **8** 1381–7
[7] Han W, Zhou Y, Zhang Y, Chen C Y, Lin L, Wang X, Wang S and Wang Z L 2012 *ACS Nano* **6** 3760–6
[8] Wu W and Wang Z L 2011 *Nano Lett.* **11** 2779–85
[9] Lin L, Hu Y, Xu C, Zhang Y, Zhang R, Wen X and Wang Z L 2013 *Nano Energy* **2** 75–81
[10] Yu A, Jiang P and Wang Z L 2012 *Nano Energy* **1** 418–23
[11] Wu W, Wen X and Wang Z L 2013 *Science* **340** 952–7
[12] Wu W *et al* 2014 *Nature* **514** 470–4
[13] Liu W, Zhang A, Zhang Y and Wang Z L 2015 *Appl. Phys. Lett.* **107** 083105
[14] Chen L, Xue F, Li X, Huang X, Wang L, Kou J and Wang Z L 2016 *ACS Nano* **10** 1546–51
[15] Pan C, Dong L, Zhu G, Niu S, Yu R, Yang Q, Liu Y and Wang Z L 2013 *Nat. Photon.* **7** 752
[16] Wen X, Wu W and Wang Z L 2013 *Nano Energy* **2** 1093–100
[17] Peng M, Zhang Y, Liu Y, Song M, Zhai J and Wang Z L 2014 *Adv. Mater.* **26** 6767–72
[18] Gao Y and Wang Z L 2007 *Nano Lett.* **7** 2499–505
[19] Gao Y and Wang Z L 2009 *Nano Lett.* **9** 1103–10
[20] Zhang Y, Liu Y and Wang Z L 2011 *Adv. Mater.* **23** 3004–13
[21] Zhang Y and Wang Z L 2012 *Adv. Mater.* **24** 4712–8
[22] Liu W, Zhang A, Zhang Y and Wang Z L 2015 *Nano Energy* **14** 355–63
[23] Qin C, Gu Y, Sun X, Wang X and Zhang Y 2015 *Nano Res.* **8** 2073–81
[24] Sun X, Gu Y, Wang X, Zhang Z and Zhang Y 2015 *Phys. Status Solidi* B **252** 1767–72
[25] Sun X, Gu Y, Wang X and Zhang Y 2013 *Phys. Chem. Chem. Phys.* **15** 13070–6
[26] Dong Y and Brillson L J 2008 *J. Electron. Mater.* **37** 743–8
[27] Zhang G, Luo X, Zheng Y and Wang B 2012 *Phys. Chem. Chem. Phys.* **14** 7051–8
[28] Kresse G and Hafner J 1993 *Phys. Rev.* B **48** 13115–8
[29] Kresse G and Furthmüller J 1996 *Phys. Rev.* B **54** 11169–86
[30] Blöchl P E 1994 *Phys. Rev.* B **50** 17953–79
[31] Kresse G and Joubert D 1999 *Phys. Rev.* B **59** 1758–75
[32] Perdew J P, Burke K and Ernzerhof M 1996 *Phys. Rev. Lett.* **77** 3865–8
[33] Junquera J, Cohen M H and Rabe K M 2007 *J. Phys.: Condens. Matter* **19** 213203
[34] Zhou J, Gu Y, Fei P, Mai W, Gao Y, Yang R, Bao G and Wang Z L 2008 *Nano Lett.* **8** 3035–40
[35] Yu R, Dong L, Pan C, Niu S, Liu H, Liu W, Chua S, Chi D and Wang Z L 2012 *Adv. Mater.* **24** 3532–7
[36] Yu R, Wu W, Pan C, Wang Z, Ding Y and Wang Z L 2015 *Adv. Mater.* **27** 940–7